Measurement of yields and angular distributions of γ-quanta from the interaction of 14.1 MeV neutrons with oxygen, phosphorus and sulfur nuclei

Grozdanov D.N.
for TANGRA collaboration

The Elements of Life

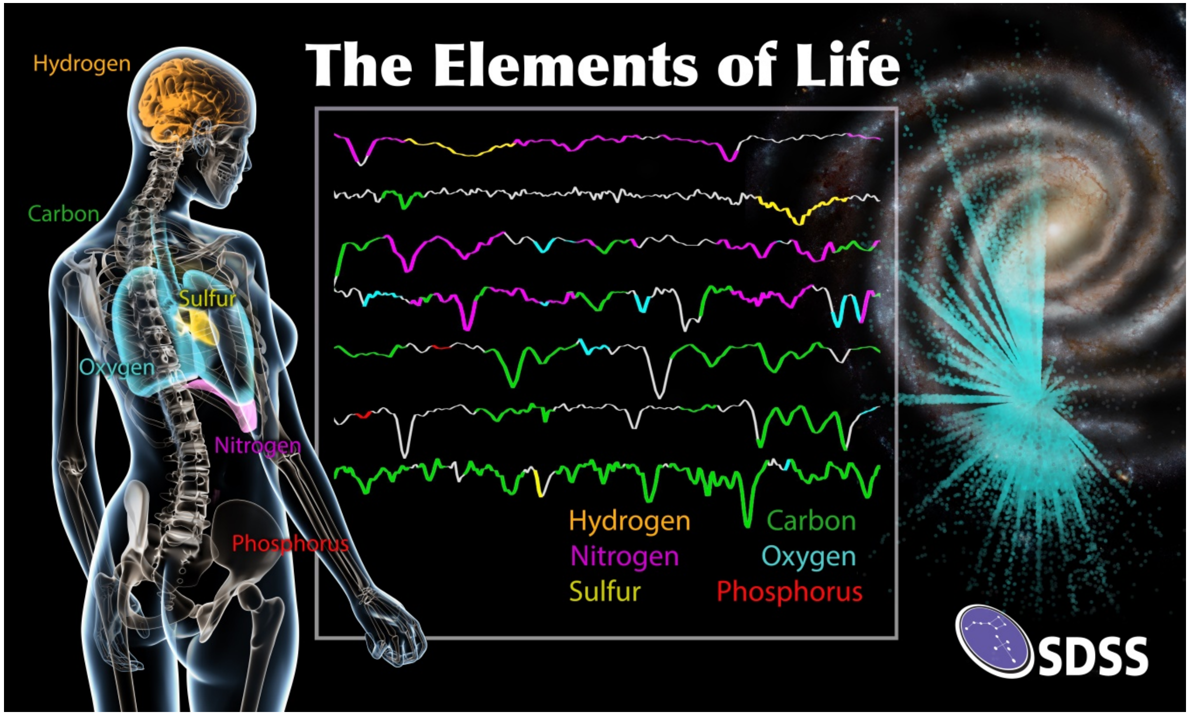

The six most common elements of life on Earth (including more than 97% of the mass of a human body) are carbon, hydrogen, nitrogen, oxygen, sulphur and phosphorus.

https://www.sdss.org/press-releases/the-elements-of-life-mapped-across-the-milky-way-by-sdssapogee/

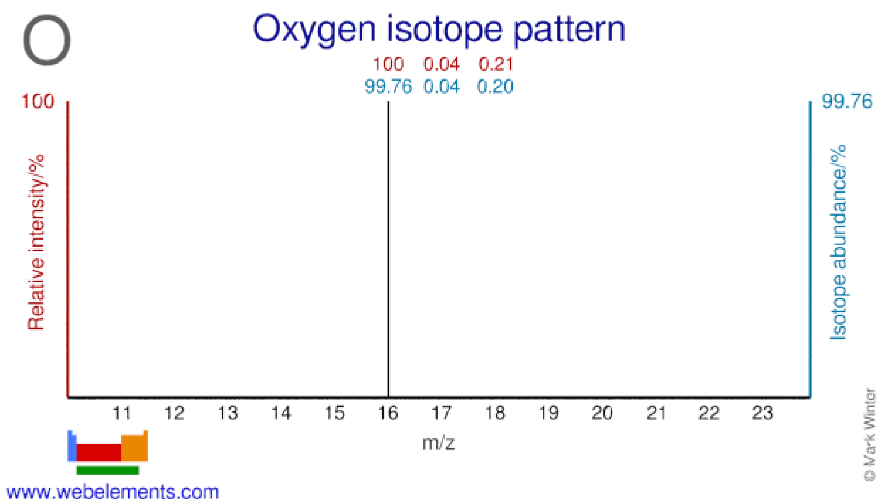
O
Oxygen isotope pattern
100 0.04 0.21
99.76 0.04 0.20
100
99.76
Relative intensity/%
Isotope abundance/%
11 12 13 14 15 16 17 18 19 20 21 22 23
m/z
www.webelements.com
© Mark Winter

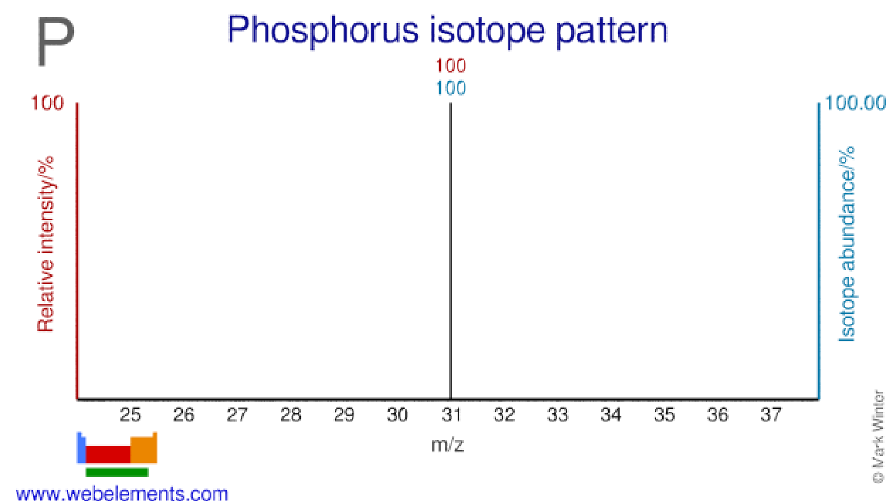
P
Phosphorus isotope pattern
100
100
100
100.00
Relative intensity/%
Isotope abundance/%
25 26 27 28 29 30 31 32 33 34 35 36 37
m/z
www.webelements.com
© Mark Winter

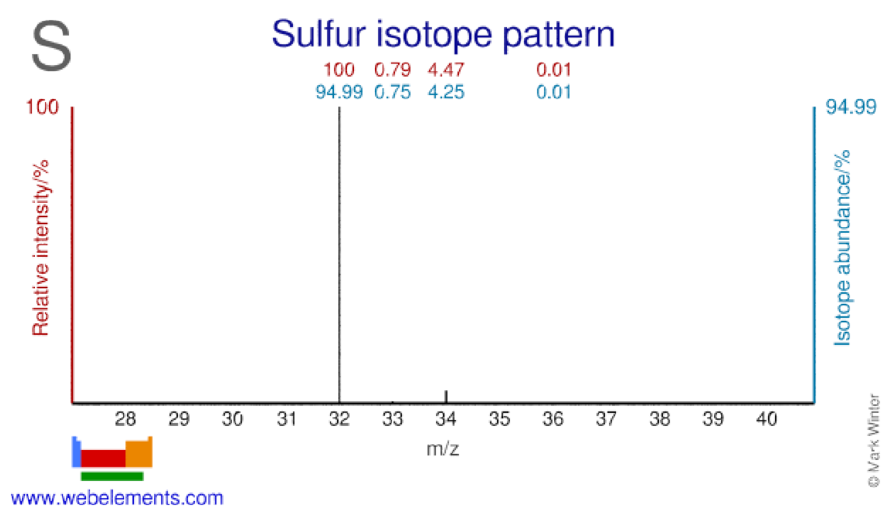
S
Sulfur isotope pattern
100 0.79 4.47 0.01
94.99 0.75 4.25 0.01
100
94.99
Relative intensity/%
Isotope abundance/%
28 29 30 31 32 33 34 35 36 37 38 39 40
m/z
www.webelements.com
© Mark Winter

TANGRA project

The project "TANGRA" (TAgged Neutrons and Gamma RAys) is devoted to study of neutron-nuclear interactions, using the tagged neutron method (TNM). The essence of TNM is to register the characteristic nuclear gamma-radiation, resulting from the interaction of neutrons from the binary d(t, 4He)n reaction with the nuclei of the substances under study, in coincidence with the accompanying alpha-particles, detected by the position-sensitive alpha-detector located inside the neutron generator vacuum chamber

TANGRA Setups

Multidetector, multipurpose, multifunctional, mobile systems, to study the characteristics of the products from the nuclear reaction induced by 14 MeV tagged neutrons. TANGRA Setups consist of a portable generator of “tagged” neutrons with energies of 14.1 MeV, ING-27, with or without an iron shield-collimator, 2D fast neutron beam profilometer, arrays of neutron-gamma detectors in geometry of daisy-flower (Romashka, Romasha, HPGe), and a computerized system for data acquisition and analysis (DAQ).

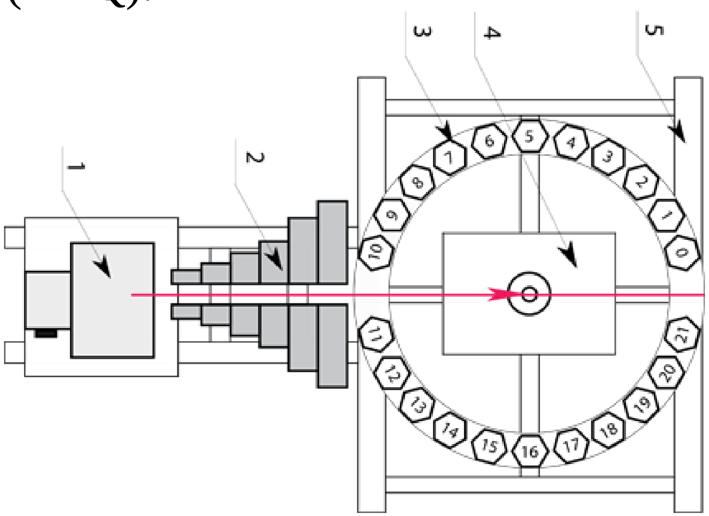

Fig. 1. NaI(Tl) Romashka consists of 22 hexagonal prism NaI(Tl) detectors with size 78 x 90 x 200 mm

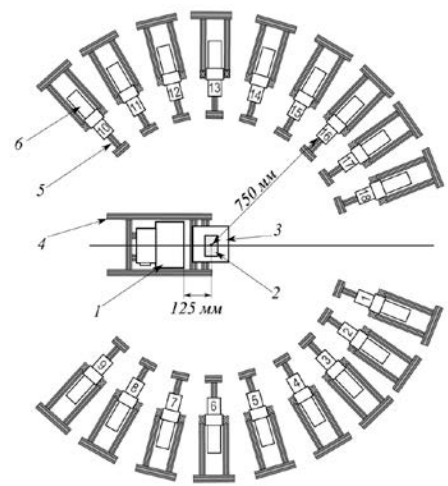

Fig. 2. BGO Romasha consists of 18 BGO detectors with size ϕ 76 x 65 mm

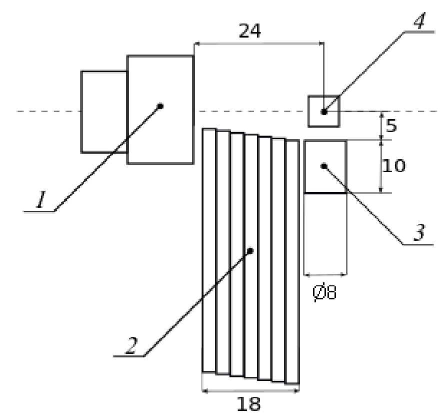

Fig. 3. HPGe Romasha, consists of a HPGe detector Ortec®GMX 30-83-PL-S, ϕ 57.5 x 66.6 mm

ING-27 Neutron Generator and Tagged Neutron Method

Main characteristics of ING-27

Continuous Mode: 14-MeV neutrons
Initial Intensity: > 5.0 x 10^7 n/s/4π
Final Intensity: > 2.5 x 10^7 n/s/4π
TiT-to-front distance : 44.0 ± 1.4 mm
TiT-to-α–detector distance: 100 ± 2 mm
Power supply voltage: 200 ± 5 V
Max Power Supply Current: 300 ± 30 mV
Consumed Power: < 40 W
Double-side Si α-particles detector
Number of pixels: 64 (8x8 strips)
Pixel area: 6x6 mm^2
Distance between strips: 0.5 mm
Voltage bias: –250V DC
Dark current: < 8μA
n-tube life-time: > 800 h
< ING Duty time >: 18 months

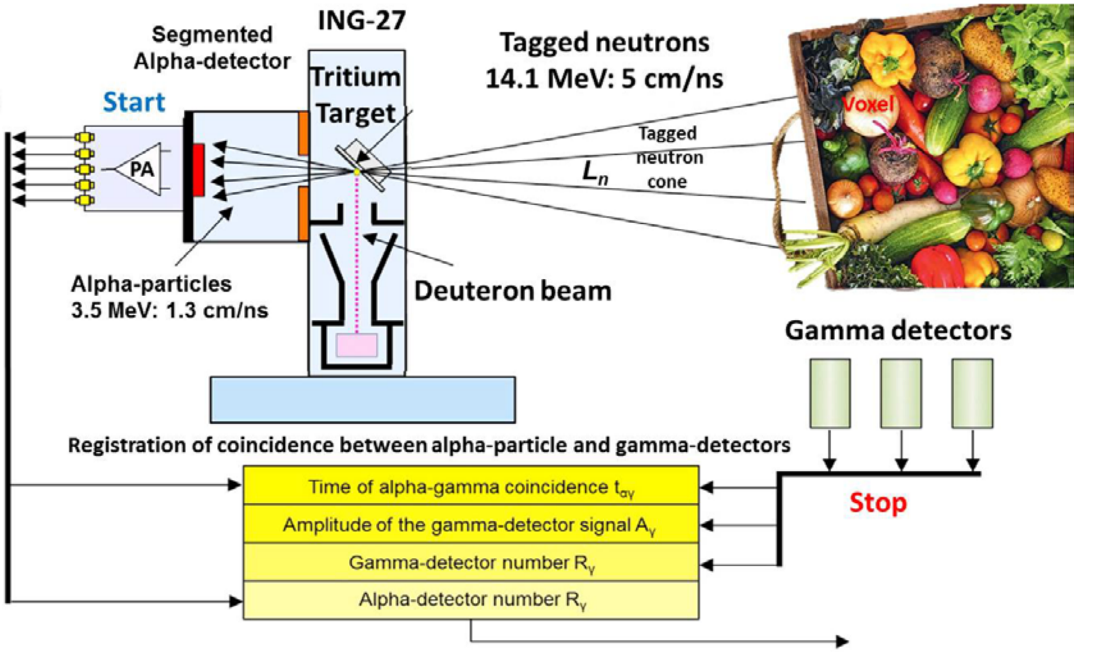

Fig. 4. Tagged Neutron Method

Measurements of tagged neutron beams’ profiles

2D-detector, made of 4 double-sided stripped position-sensitive Si-detectors

Each Si detector consists of 32x32 strips ~1.8 mm thick
Size of one detector: 60x60 mm

Total size: 120x120 mm
Thickness: 300 μm
Neutron detection efficiency: ~0.8%
At this stage each 8 strips are grouped together
forming a matrix 8x8 with a pixel size of ~1.5x1.5 cm

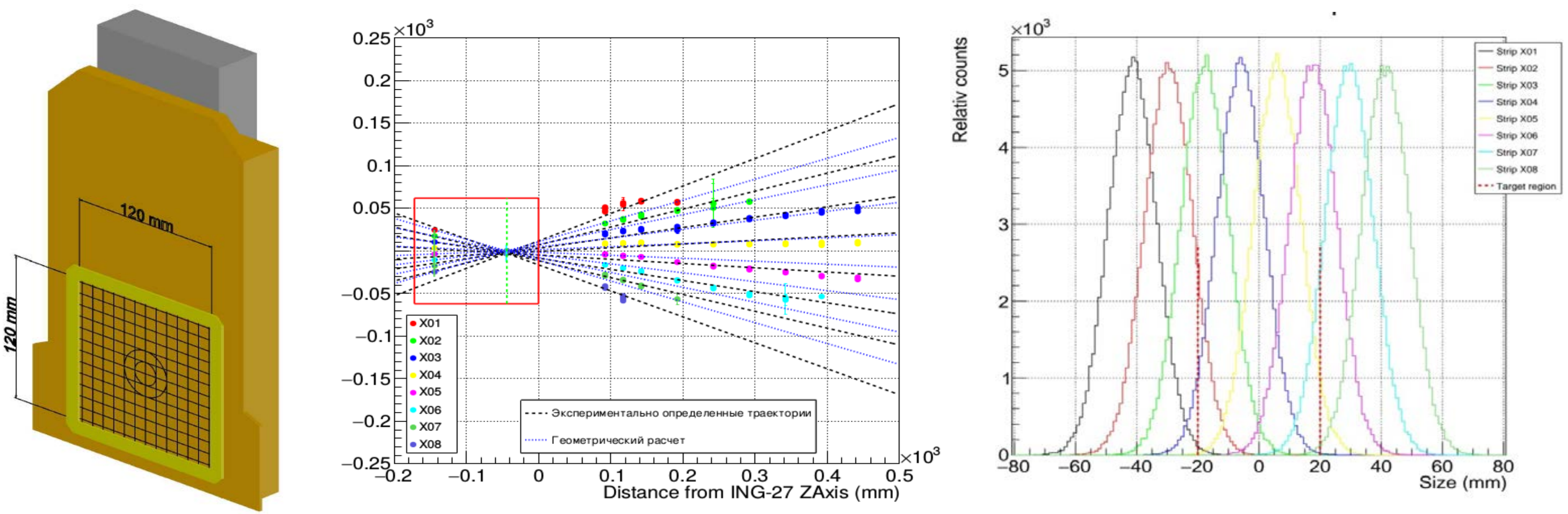

Fig. 5. 2D-detector and Measurements of tagged neutron beams profiles

HPGe Analysis

N	E_γ (keV)	Reaction	Cross section σ (mb)
1	140	Background	-
2	169.3	$^{16}O(n,a)^{13}C$	23.1
3	200	Background	-
4	298.2	$^{16}O(n,p)^{16}N$	22.5

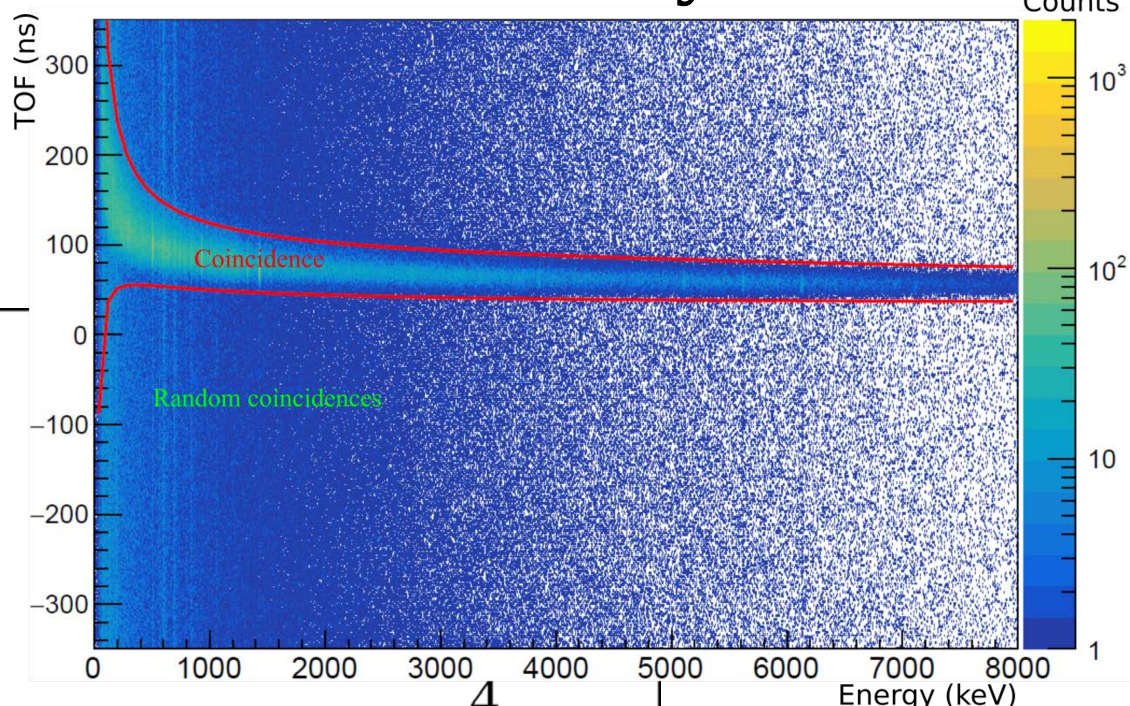

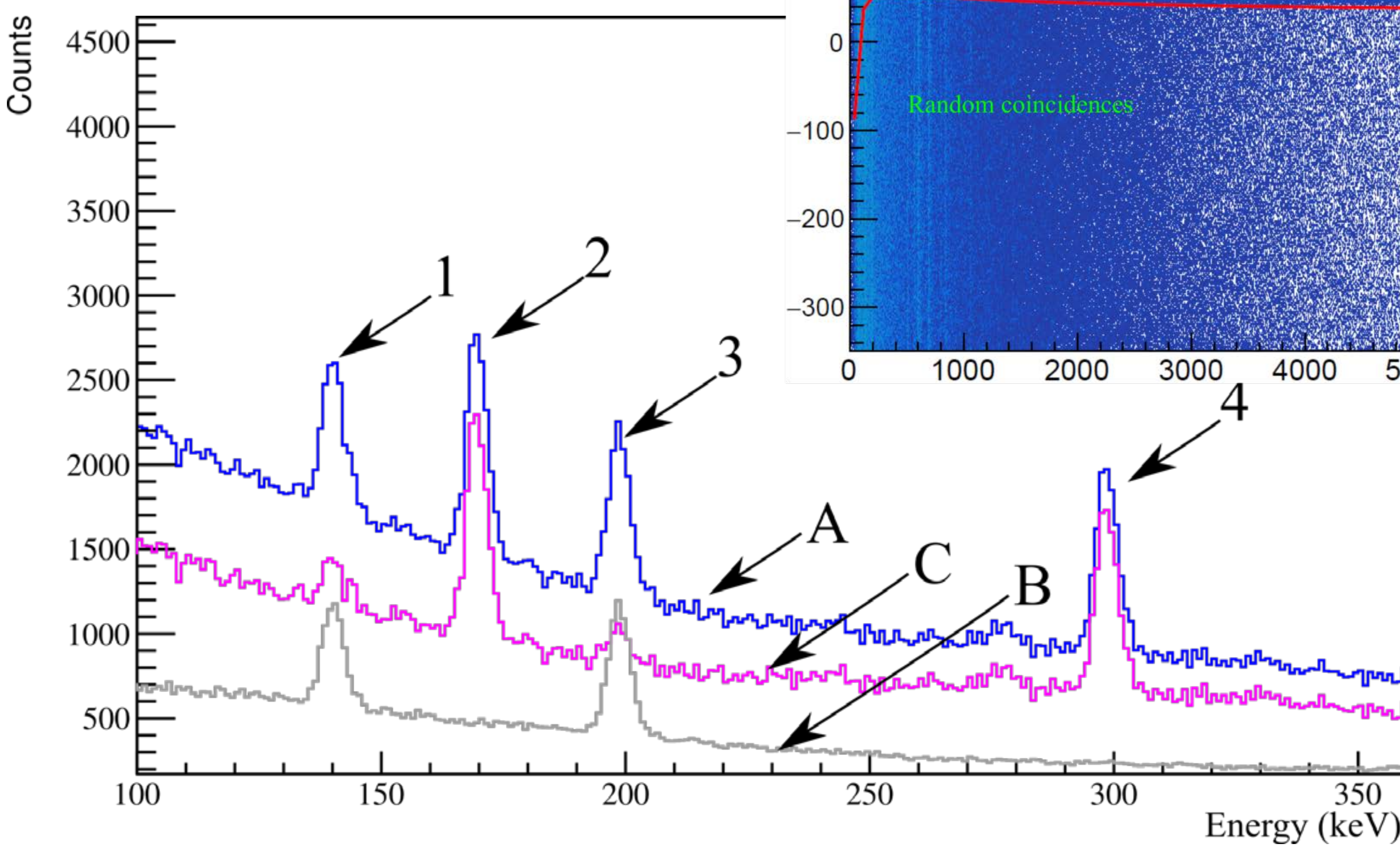

A – Coincidence
B – Random coincidence
C – Difference (pure) spectrum (A – B)

BGO Analyze

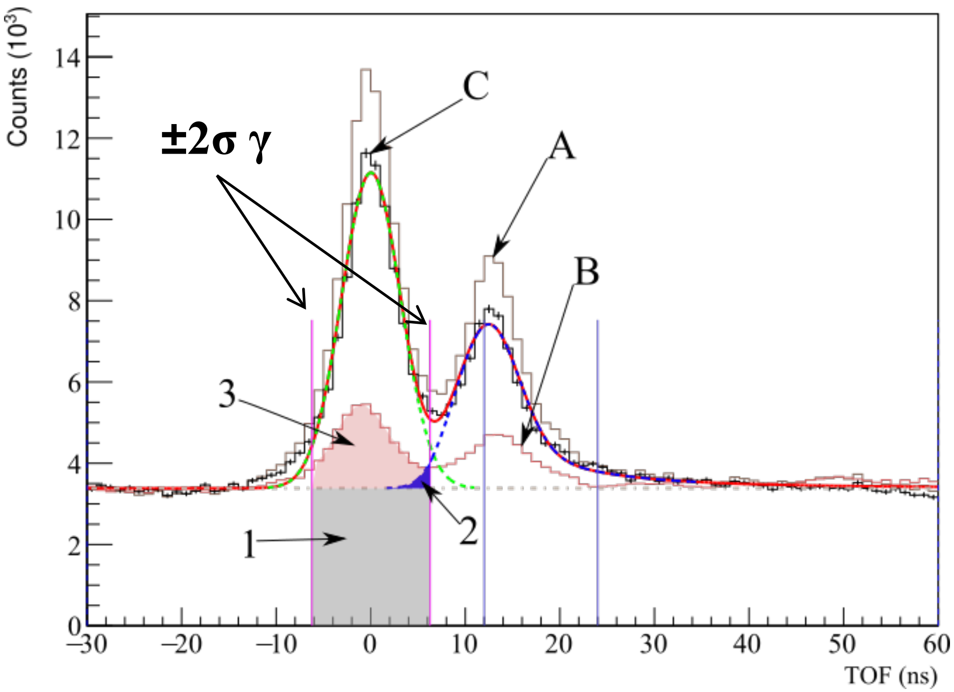

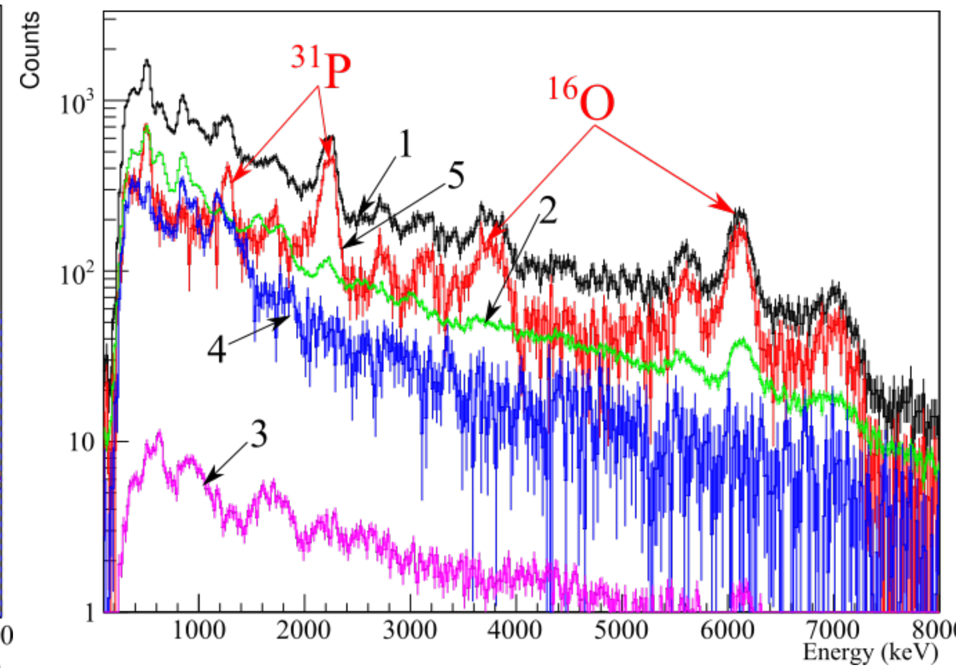

A – Full spectrum from sample
B – Background (not sample)
C – Difference (pure) spectrum (A – B)

1 – Full spectrum from sample
2 – Background from neutrons scattered on the sample and the immediate environment
3 – Background from γ quanta produced by the interaction of neutrons with the nearest environment of the sample

1 – Full spectrum from sample in the gamma window ±2σ γ
2 – Random coincidence background
3 – Background from neutrons
4 – Background from gamma rays (from 3 in time spectra)
5 - Pure spectrum (for subtraction of all backgrounds)

Response function of BGO scintillation detectors

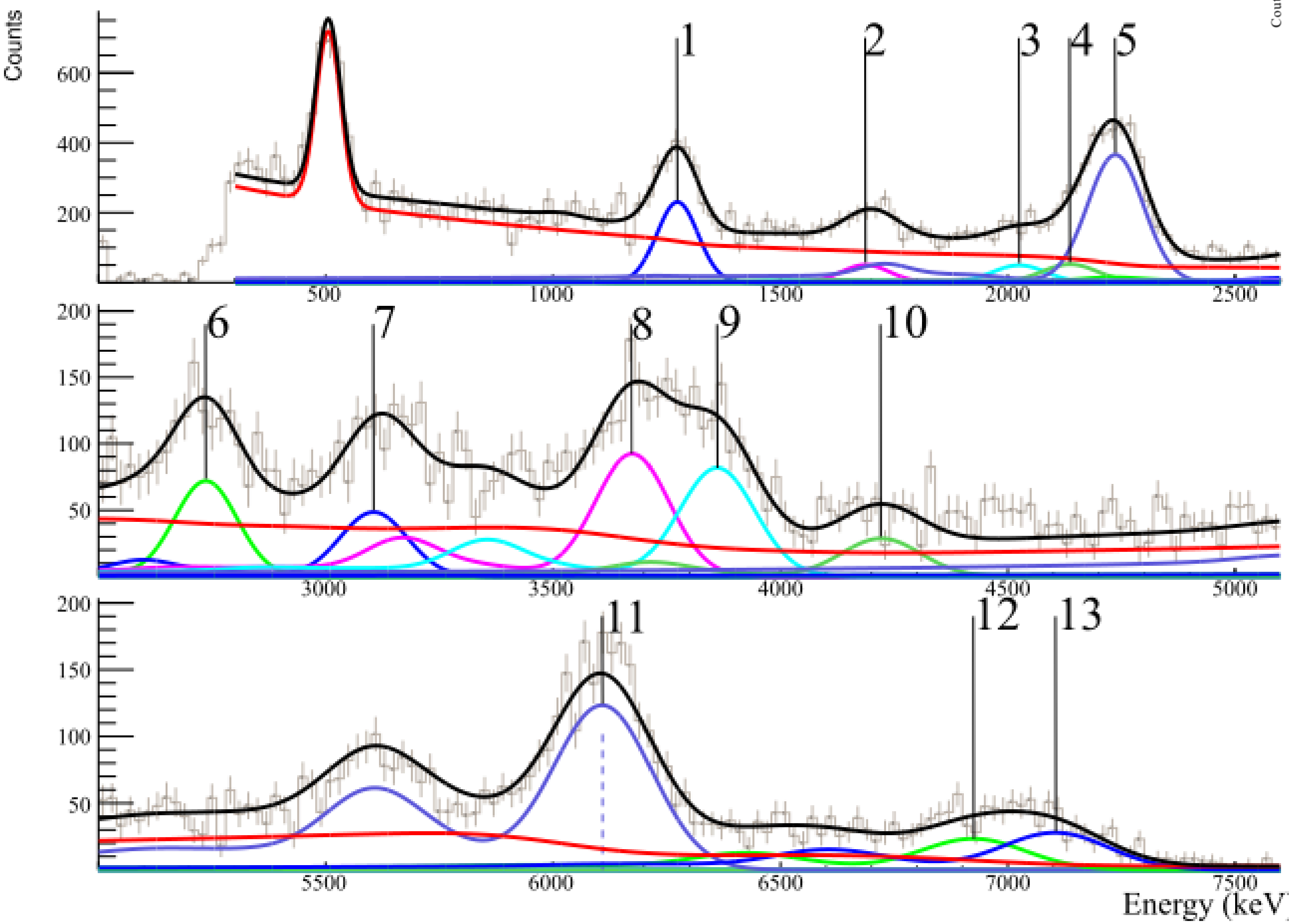

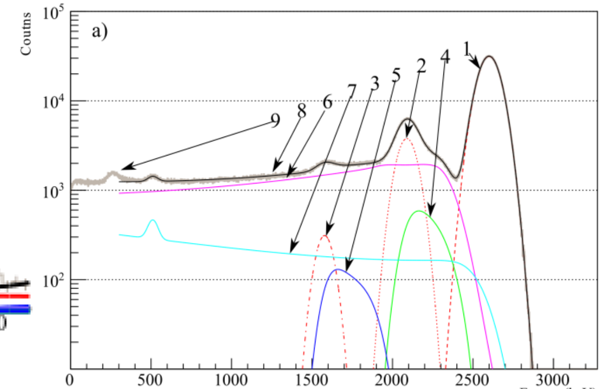

Grozdanov, D.N., at all. NIM A, 2021, https://doi.org/10.1016/j.nima.2021.165741

$$f_\theta(E) = \sum_j Y_j \cdot R\left(E_\gamma^j, E\right) + A_b + \exp(B_b + C_b E)$$

N	E_γ (keV)	Reaction	Cross section σ (mb)
1	1266.2	$^{31}P(n,n')^{31}P$	128.5
2	1649.9	$^{31}P(n,n')^{31}P$	20.7
3	2028.9	$^{31}P(n,n')^{31}P$	38.9
4	2148.4	$^{31}P(n,n')^{31}P$	22.5
5	2233.6	$^{31}P(n,n')^{31}P$	58.0
6	2742.0	$^{16}O(n,n')^{16}O$	50.7
7	3089.4	$^{16}O(n,\alpha)^{13}C$	29.9
8	3684.5	$^{16}O(n,\alpha)^{13}C$	72.9
9	3853.8	$^{16}O(n,\alpha)^{13}C$	39.8
10	4179.6	$^{16}O(n,n')^{16}O$	9.8
11	6129.9	$^{16}O(n,n')^{16}O$	144.4
12	6917.1	$^{16}O(n,n')^{16}O$	119.7
13	7116.9	$^{16}O(n,n')^{16}O$	47.0

Energies of γ transitions E_γ (keV) observed upon irradiating oxygen nuclei with 14.1 MeV neutrons

E_γ (keV)	Reaction	J_i^P (E_i, keV)	J_j^P (E_j, keV)	Y_γ, %			
				This work	TALYS	[1]	[2]
169.3	$^{16}O(n,a)^{13}C$	$\frac{5}{2}^{+}$(3853.8)	$\frac{3}{2}^{-}$(3684.5)	32.0 (3.6)	16.0		
298.2	$^{16}O(n,p)^{16}N$	3^{-}(298.2)	2^{-}(0)	42.2 (3.8)	15.6		
987.0	$^{16}O(n,n')^{16}O$	1^{-}(7116.8)	3^{-}(6129.9)	-	-	4.2 (0.8)	
1755.1	$^{16}O(n,n')^{16}O$	2^{-}(8871.9)	1^{-}(7116.8)	-	5.2	4.6 (0.9)	
1954.8	$^{16}O(n,n')^{16}O$	2^{-}(8871.9)	2^{-}(6917.1)	-	1.6	4.1 (2.6)	
2208.1	$^{16}O(n,n')^{16}O$	3^{+}(11080.0)	2^{+}(8871.9)	4.8 (1.4)	16.8		
2742.0	**$^{16}O(n,n')^{16}O$**	**2^{-}(8871.9)**	**3^{-}(6129.9)**	**32.0 (4.0)**	**35.1**	**25.7 (3.2)**	**31.3 (7.0)**
3089.4	$^{16}O(n,\alpha)^{13}C$	$\frac{1}{2}^{+}$(3089.4)	$\frac{1}{2}^{-}$(0)	-	20.7	14.9 (1.7)	
3684.5	**$^{16}O(n,\alpha)^{13}C$**	**$\frac{3}{2}^{-}$(3684.5)**	**$\frac{1}{2}^{-}$(0)**	**35.1 (6.2)**	**50.5**	**38.9 (4.5)**	**29.6 (6.2)**
3853.8	**$^{16}O(n, \alpha)^{13}C$**	**$\frac{5}{2}^{+}$(3853.8)**	**$\frac{1}{2}^{-}$(0)**	**29.9 (3.7)**	**27.6**	**22.8 (3.3)**	**23.5 (4.9)**
4438.9	$^{16}O(n,n'\alpha)^{12}C$	2^{+}(4438.9)	0^{+} (0)	-	-	11.6 (1.7)	
6129.9	**$^{16}O(n,n')^{16}O$**	**3^{-}(6129.9)**	**0^{+} (0)**	**100**	**100**	**100**	**100**
6917.1	$^{16}O(n,n')^{16}O$	2^{+}(6917.1)	0^{+} (0)	31.0 (3.8)	82.9	31.8 (3.7)	34.8 (7.3)
7116.9	$^{16}O(n,n')^{16}O$	1^{-}(7116.8)	0^{+} (0)	33.5 (4.9)	32.6	36.1 (4.4)	39.1 (8.4)

[1] Simakov S. P., Pavlik A., Vonach H. et al. Status of Experimental and Evaluated Discrete Gamma-Ray Production at En=14.5 MeV / International Atomic Energy Agency, Vienna, Austria. 1998.
[2] Nyberg-Ponnert K., Jönsson B., Bergqvist I. Gamma Rays Produced by the Interaction of 15 MeV Neutrons in N, O, Mg and Al // Phys. Scripta. 1971. Vol. 4, no. 4/5. P. 165—173.

Energies of γ transitions E_γ (keV) observed upon irradiating phosphorus nuclei with 14.1 MeV neutrons

E_γ (keV)	Reaction	J_i^P (E_i, keV)	J_j^P (E_j, keV)	Y_γ, %		
				This work	TALYS	[1]
752.2	$^{31}P(n,p)^{31}Si$	$\frac{1}{2}^+$ (752.2)	$\frac{3}{2}^+$ (0)	5.7 (2.3)	4.6	
983.0	$^{31}P(n,\alpha)^{28}Al$	3^+(1013.6)	2^+(30.6)	4.6 (1.0)	6.4	
1136.2	$^{31}P(n,n')\,^{31}P$	$\frac{7}{2}^-$ (4431.2)	$\frac{5}{2}^+$ (3295.0)	7.7 (1.4)	2.2	
1263.3 **1266.1**	**$^{31}P(n,d)^{30}Si$** **$^{31}P(n,n')\,^{31}P$**	**2^+(3498.5)** **$\frac{3}{2}^+$ (1266.1)**	**2^+(2235.3)** **$\frac{1}{2}^+$ (0)**	**72.8 (11.6)**	**5.0** **53.7**	**43.8 (10.6)**
1694.9	$^{31}P(n,p)^{31}Si$	$\frac{5}{2}^+$ (1694.9)	$\frac{7}{2}^+$ (0)	12.4 (2.5)	8.6	
1928.3	$^{31}P(n,n')\,^{31}P$	$\frac{9}{2}^+$ (5342.9)	$\frac{7}{2}^+$ (3414.6)	6.1 (1.9)	3.9	
2148.5	$^{31}P(n,n')\,^{31}P$	$\frac{7}{2}^+$ (3414.6)	$\frac{3}{2}^+$ (1266.1)	17.6 (3.5)	16.3	14.6 (3.3)
2197.6	$^{31}P(n,n')\,^{31}P$	$\frac{7}{2}^-$ (4431.2)	$\frac{5}{2}^+$ (2233.6)	6.0 (1.2)	2.9	
2233.6 **2235.3** **2240.0**	**$^{31}P(n,n')\,^{31}P$** **$^{31}P(n,d)^{30}Si$** **$^{31}P(n,n')\,^{31}P$**	**$\frac{5}{2}^+$ (2233.6)** **2^+(2235.3)** **$\frac{3}{2}^+$ (3506.1)**	**$\frac{1}{2}^+$ (0)** **0^+ (0)** **$\frac{3}{2}^+$ (1266.1)**	**100**	**24.3** **100** **3.8**	**100**
3658.3	$^{31}P(n,n')\,^{31}P$	$\frac{9}{2}^+$ (5891.9)	$\frac{5}{2}^+$ (2233.6)	13.8 (3.3)	1.6	

[1] Simakov S. P., Pavlik A., Vonach H. et al. Status of Experimental and Evaluated Discrete Gamma-Ray Production at En=14.5 MeV / International Atomic Energy Agency, Vienna, Austria. 1998.

Energies of γ transitions E_γ (keV) observed upon irradiating sulfur nuclei with 14.1 MeV neutrons

E_γ (keV)	Reaction	J_i^P (E_i, keV)	J_j^P (E_j, keV)	Y_γ, %		
				This work	TALYS	[1]
1266.1 **1273.4**	**$^{32}S(n,d)^{31}P$** **$^{32}S(n,\alpha)^{29}Si$**	**$\frac{3}{2}^+$ (1266.1)** **$\frac{3}{2}^+$ (1273.4)**	**$\frac{1}{2}^+$ (0)**	**47.9 (1.9)**	**46.1** **41.7**	**43.6 (7.0)**
1320.2 **1322.8**	$^{34}S(n,n')^{34}S$ $^{32}S(n,p)^{32}P$	3^-(4624.4) 2^+(1322.8)	2^+(3304.2) 1^+(0)	10.8 (3.4)	1.7 8.5	
1676.9	$^{32}S(n,p)^{32}P$	3^+(1755.0)	2^+(78.1)	26.1 (1.1)	24.2	
2028.2	**$^{32}S(n,\alpha)^{29}Si$**	**$\frac{5}{2}^+$ (2028.2)**	**$\frac{1}{2}^+$ (0)**	**18.4 (1.4)**	**49.1**	
2127.8 **2228.5** **2230.6** **2233.6**	**$^{32}S(n,p)^{32}P$** **$^{32}S(n,n')^{32}S$** **$^{32}S(n,n')^{32}S$** **$^{32}S(n,d)^{31}P$**	**2^+(2217.8)** **4^+(4459.1)** **2^+(2230.6)** **$\frac{5}{2}^+$ (2233.6)**	**1^+(0)** **2^+(2230.6)** **0^+(0)** **$\frac{1}{2}^+$ (0)**	**100**	**2.5** **12.1** **100** **13.7**	**39.5 (9.6)** **100**
2775.6	**$^{32}S(n,n')^{32}S$**	**3^-(5006.2)**	**2^+ (2230.6)**	**18.5 (1.2)**	**22.9**	**14.8 (2.4)**

Yields > 10%

[1] Simakov S. P., Pavlik A., Vonach H. et al. Status of Experimental and Evaluated Discrete Gamma-Ray Production at En=14.5 MeV / International Atomic Energy Agency, Vienna, Austria. 1998.

Energies of γ transitions E_γ (keV) observed upon irradiating sulfur nuclei with 14.1 MeV neutrons

E_γ (keV)	Reaction	J_i^P (E_i, keV)	J_j^P (E_j, keV)	Y_γ, %		
				This work	TALYS	[1]
636.7	$^{32}S(n,p)^{32}P$	1^+(1149.4)	0^+(512.7)	5.6 (1.0)	12.4	
754.8	$^{32}S(n,\alpha)^{29}Si$	$\frac{5}{2}^+$ (2028.2)	$\frac{3}{2}^+$ (1273.4)	2.4 (0.8)	3.1	
1039.0	$^{32}S(n,\alpha)^{29}Si$	$\frac{5}{2}^+$ (3067.1)	$\frac{5}{2}^+$ (2028.2)	1.2 (0.4)	2.3	
1071.3	$^{32}S(n,p)^{32}P$	1^+(1149.4)	2^+(78.1)	2.1 (0.4)	10.7	
1176.7	$^{34}S(n,n')^{34}S$	2^+(3304.2)	2^+(2127.6)	2.3 (0.4)	2.4	
1244.8	$^{32}S(n,p)^{32}P$	2^+(1322.8)	2^+(78.1)	4.5 (0.5)	5.8	
1595.3	$^{32}S(n,\alpha)^{29}Si$	$\frac{7}{2}^-$ (3623.5)	$\frac{5}{2}^-$ (2028.2)	6.8 (0.5)	14.5	
1755.4	$^{32}S(n,n')^{32}S$	5^-(6761.6)	3^- (5006.2)	2.8 (0.5)	1.8	
1793.7	$^{32}S(n,\alpha)^{29}Si$	$\frac{5}{2}^+$ (3067.1)	$\frac{3}{2}^+$ (1273.4)	3.7 (0.8)	10.9	
2099.1	$^{32}S(n,p)^{32}P$	3^+(2177.2)	2^+ (78.1)	3.5 (0.4)	7.6	
2127.6	$^{34}S(n,n')^{34}S$	2^+(2127.6)	0^+ (0)	5.0 (0.4)	11.1	
3128.0	$^{32}S(n,n')^{32}S$	3^+(5412.6)	2^+ (2230.6)	4.2 (1.1)	3.7	
4180.4	$^{32}S(n,n')^{32}S$	4^+(6411.0)	2^+ (2230.6)	3.5 (1.1)	2.9	
4281.8	$^{32}S(n,n')^{32}S$	2^+(4281.8)	0^+ (0)	5.7 (1.0)	6.8	
5796.8	$^{32}S(n,n')^{32}S$	1^-(5796.8)	0^+ (0)	3.0 (0.7)	1.1	

Yields < 10%

[1] Simakov S. P., Pavlik A., Vonach H. et al. Status of Experimental and Evaluated Discrete Gamma-Ray Production at En=14.5 MeV / International Atomic Energy Agency, Vienna, Austria. 1998.

Gamma-ray Angular Distribution for Oxygen

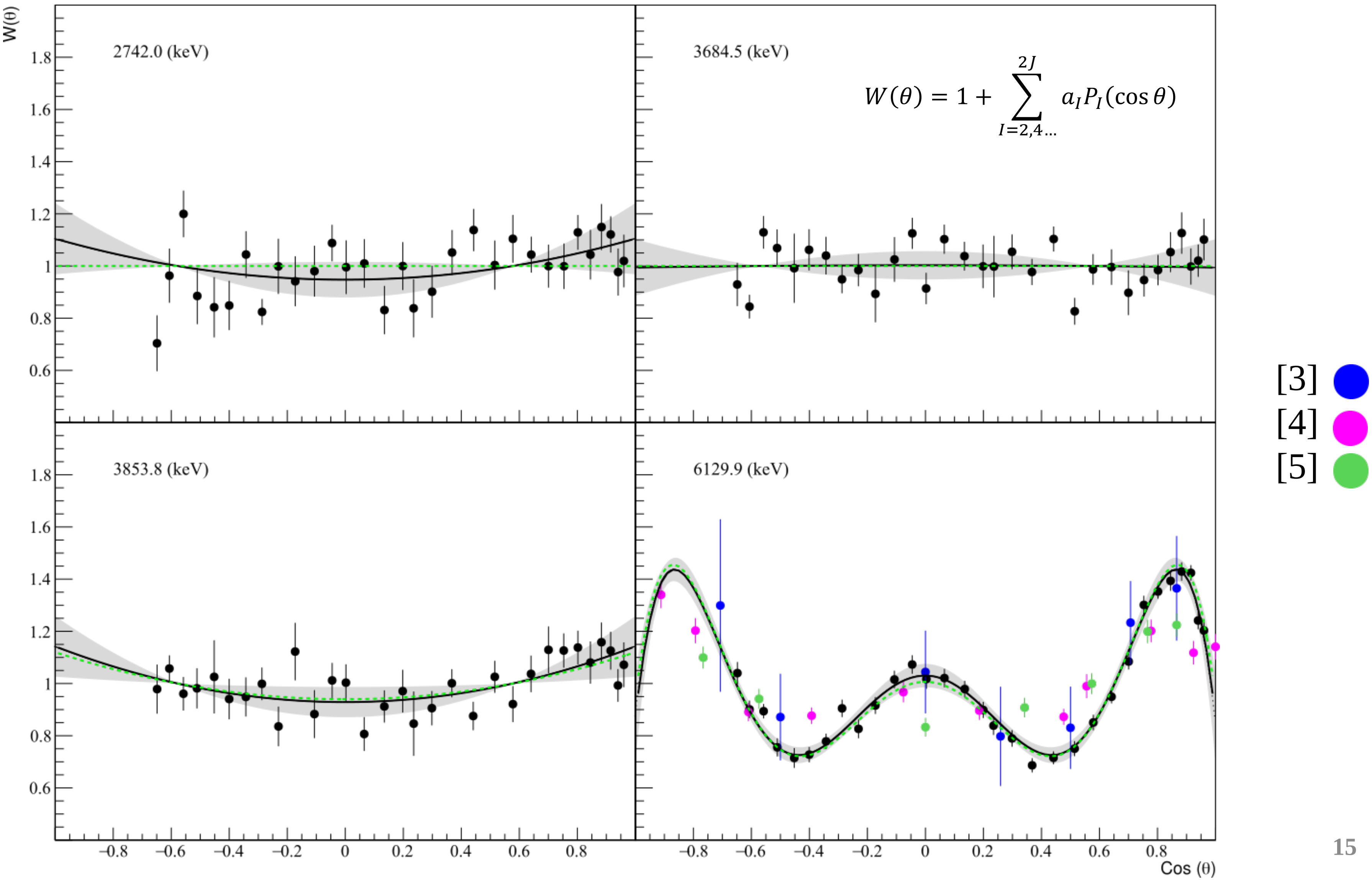

Coefficients of expansion over Legendre polynomials for angular distribution of γ quanta emitted in interaction between 14.1 MeV neutrons and Oxygen nuclei

E_γ (keV)	Reaction	J_i^P (E_i, keV)	J_j^P (E_j, keV)	Reference	α_2	α_4	α_6
2742.0	**$^{16}O(n,n')^{16}O$**	**2^-(8871.9)**	**3^-(6129.9)**	**This work**	**0.10 ± 0.04**		
3684.5	**$^{16}O(n,\alpha)^{13}C$**	**$\frac{3}{2}^-$ (3684.5)**	**$\frac{1}{2}^-$ (0)**	**This work**	**-0.01 ± 0.04**		
3853.8	**$^{16}O(n,\alpha)^{13}C$**	**$\frac{5}{2}^+$ (3853.8)**	**$\frac{1}{2}^-$ (0)**	**This work** **ENDF/B-8 [6]**	**0.14 ± 0.03** **0.12**		
6129.9	**$^{16}O(n,n')^{16}O$**	**3^-(6129.9)**	**0^+ (0)**	**This work** **Kozlowski1965 [3]** **Morgan1964 [4]** **McDonald1966 [5]** **ENDF/B-8**	**0.36 ± 0.02** **0.18 ± 0.06** **0.35 ± 0.07** **0.26 ± 0.04** **0.40**	**0.08 ± 0.02** **-0.27 ± 0.08** **0.02 ± 0.08** **0.06 ± 0.05** **0.09**	**-0.57 ± 0.03** **-0.68 ± 0.08** **-0.03 ± 0.08** **-0.21 ± 0.05** **-0.55**

[3] T. Kozlowski, W. Kusch, and J. Wojtkowska, http://cdfe.sinp.msu.ru/cgi-bin/exf2htm?-LINK=30081004;
[4] T. L. Morgan, J. B. Ashe, and D. O. Nellis, http://cdfe.sinp.msu.ru/cgi-bin/exf2htm?-LINK=12695006.
[5] W. J. McDonald, J. M. Robson, and R. Malcolm, Nucl. Phys. 75, 353 (1966);
[6] Evaluated Nuclear Data File (ENDF), https://www-nds.iaea.org/exfor/endf.htm

$$W(\theta) = 1 + \sum_{I=2,4\ldots}^{2J} a_I P_I(\cos\theta)$$

Gamma-ray Angular Distribution for Phosphorus

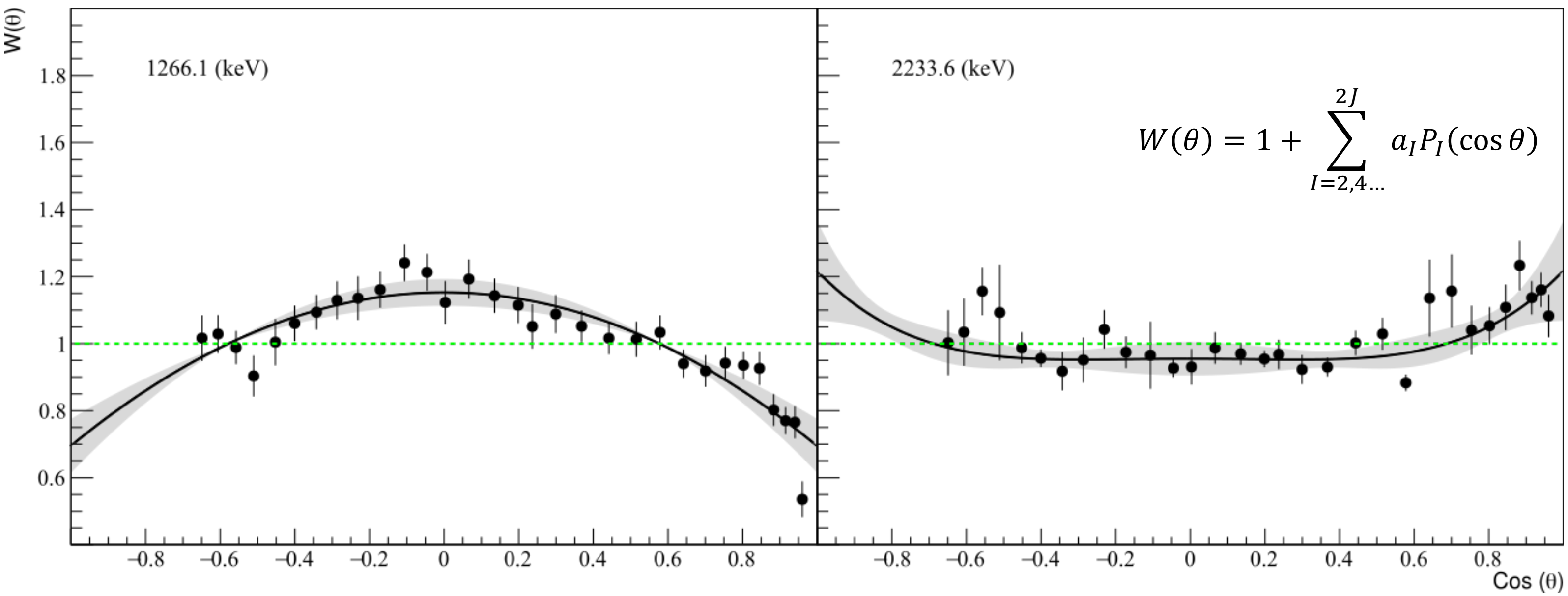

E_γ (keV)	Reaction	J_i^P (E_i, keV)	J_j^P (E_j, keV)	Reference	α_2	α_4
1263.3 1266.1	$^{31}P(n,d)^{30}Si$ $^{31}P(n,n')\,^{31}P$	2^+(3498.5) $\frac{3}{2}^+$ (1266.1)	2^+(2235.3) $\frac{1}{2}^+$ (0)	This work	-0.31 ± 0.02	*
2233.6 2235.3 2240.0	$^{31}P(n,n')\,^{31}P$ $^{31}P(n,d)^{30}Si$ $^{31}P(n,n')\,^{31}P$	$\frac{5}{2}^+$ (2233.6) 2^+(2235.3) $\frac{3}{2}^+$ (3506.1)	$\frac{1}{2}^+$ (0) 0^+ (0) $\frac{3}{2}^+$ (1266.1)	This work	0.14 ± 0.02	0.07 ± 0.03

Gamma-ray Angular Distribution for Sulfur

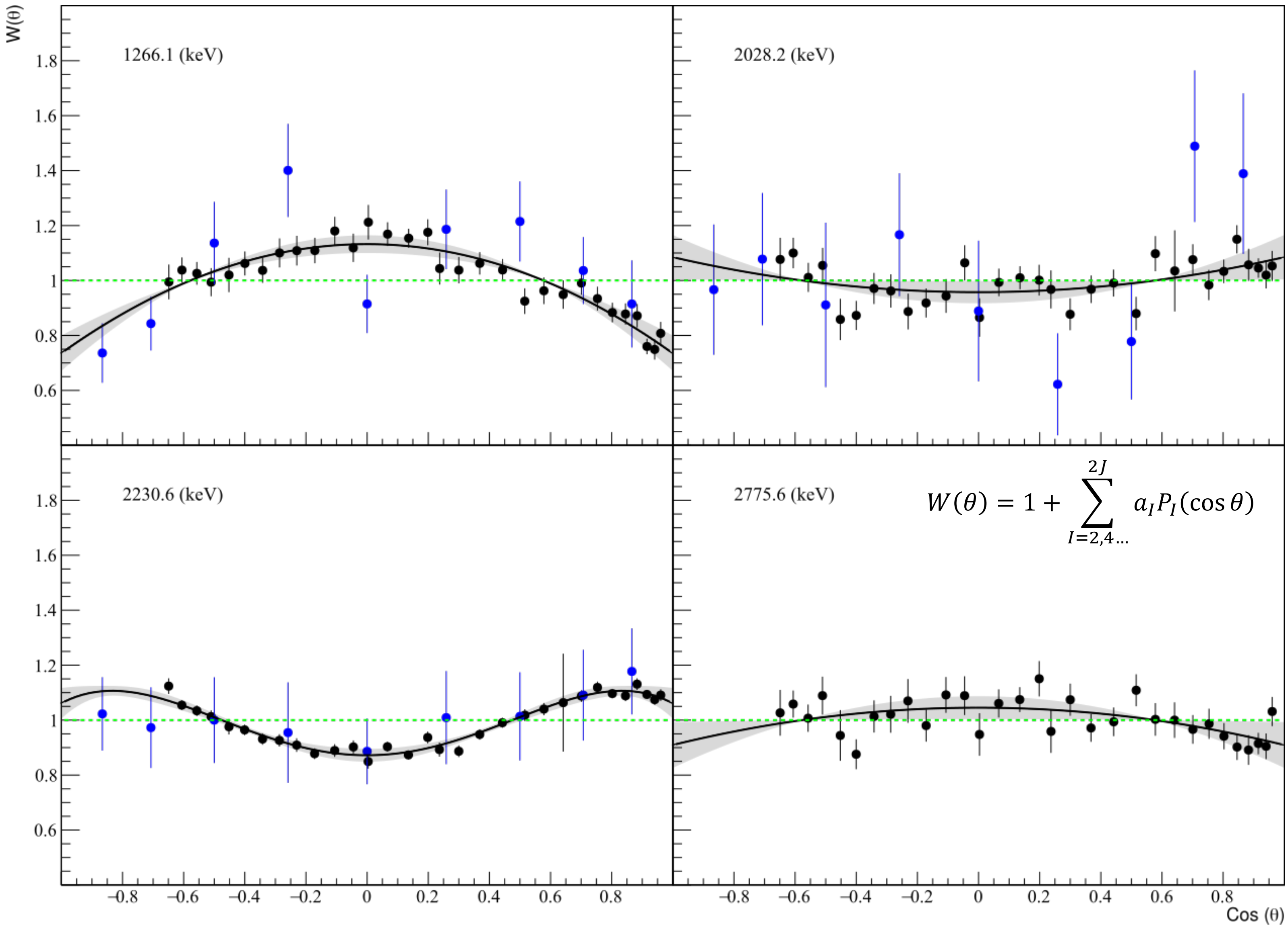

$$W(\theta) = 1 + \sum_{I=2,4...}^{2J} a_I P_I(\cos\theta)$$

[7] ●

Coefficients of expansion over Legendre polynomials for angular distribution of γ quanta emitted in interaction between 14.1 MeV neutrons and Sulfur nuclei

E_γ (keV)	Reaction	J_i^P (E_i, keV)	J_j^P (E_j, keV)	Reference	α_2	α_4
1266.1 1273.4	**$^{32}S(n,d)^{31}P$** $^{32}S(n,\alpha)^{29}Si$	**$\frac{3}{2}^+$ (1266.1)** $\frac{3}{2}^+$ (1273.4)	$\frac{1}{2}^+$ (0)	This work **Abbodanno1973 [7]**	-0.26 ± 0.02 **-0.28 ± 0.13**	*
2028.2	$^{32}S(n,\alpha)^{29}Si$	$\frac{5}{2}^+$ (2028.2)	$\frac{1}{2}^+$ (0)	This work **Abbodanno1973 [7]**	0.08 ± 0.02 **0.35 ± 0.20**	*
2127.8 2228.5 **2230.6** 2233.6	$^{32}S(n,p)^{32}P$ $^{32}S(n,n')^{32}S$ **$^{32}S(n,n')^{32}S$** $^{32}S(n,d)^{31}P$	2^+(2217.8) 4^+(4459.1) **2^+(2230.6)** $\frac{5}{2}^+$ (2233.6)	1^+(0) 2^+(2230.6) **0^+(0)** $\frac{1}{2}^+$ (0)	This work **Abbodanno1973 [7]**	0.17 ± 0.01 **0.13 ± 0.05**	-0.11 ± 0.01 **-0.04 ± 0.08**
2775.6	$^{32}S(n,n')^{32}S$	3^-(5006.2)	2^+ (2230.6)	This work	-0.09 ± 0.02	*

[7] U. Abbondanno, R. Giacomich, M. Lagonegro, and G. Pauli, J. Nucl. Energy 27, 227 (1973).

$$W(\theta) = 1 + \sum_{I=2,4\dots}^{2J} a_I P_I(\cos\theta)$$

CONCLUSIONS

Using the Target Neutron Method (TNM) we reduced the radiation background in the collected pulse-height spectra by ~70% and improved scientifically the quality of the experimental data.

The energies of observed γ transitions were determined, and the yields of γ quanta for transitions formed upon irradiating oxygen, phosphorus and sulfur with 14.1 MeV neutrons were measured.

Our data generally agree with those in the literature. The experimental data for (n,n'γ) reactions on ^{16}O, ^{31}P and ^{32}S isotopes are in good agreement among themselves and with model calculations using the TALYS 1.9 code.

Substantial discrepancies are observed in both model calculations and experimental data for reactions with the emission of other particles (protons, deuterons, and α particles).

Thank you for your attention